

Laboratory Model Tests with Silicone Rubber Ground Model (Embedment Effect Test on Soil-Structure Interaction)

Ryoichi SHOHARA, Akira MITA
Shimizu Corporation, Tokyo, Japan

Masanori IZUMI
Tohoku University, Sendai, Japan

Kinji AKINO
Nuclear Power Engineering Center, Tokyo, JAPAN

1 INTRODUCTION

A seismic response analysis of a building considering the effects of soil-structure interaction has become common even for the buildings with embedded foundations. However, experimental data to verify the analysis tools are still very few. Model tests were carried out using ground models made of silicone rubber (soft and hard ground models) to investigate the embedment effects experimentally and to verify the seismic analysis codes used in the design of embedded reactor buildings in Japan. An aluminum structure model was installed in a pit of the ground model and impulse hammering and shaking table test were conducted for several embedment depths.

This paper presents outline of these tests and some of the test results. The companion paper (Moriyama, K. et al. 1991) discusses the comparison between tests and analyses.

2 OUTLINE OF TEST

The ground and foundation models are shown in figure 1. Two ground models of the same size were provided. One ground model is made of soft silicone rubber and the other is made of hard silicone rubber. Their material constants are shown in Table 1. Each ground model has a cylindrical shape with diameter of 300cm and height of 70cm, and has an 18cm deep pit at its center. They have brass bars around their circumferential edges to restrict vertical deformation of ground models during shaking table test.

Two building models of the same configuration and materials were also provided. They have rigid square foundations (30x30x18cm). The second and roof slabs are made of aluminum as shown in figure 2. They also have columns made of spring phosphor bronze. The dimensions are chosen considering typical site conditions and reactor buildings in Japan. Ground-foundation tests and ground-building tests were conducted for each ground model. A foundation was installed in the pit of the ground model and impulse hammering and shaking table test were conducted for three embedment depths (0cm, 9cm and 18cm) in case of the soft ground model and for two embedment depths (0cm, 18cm) in case of the hard ground model.

Hammering tests were carried out to determine the vibration characteristics of the building model, and to evaluate the vibration characteristics of the ground-foundation interaction system and the ground-building interaction system. Excitation was applied with an impulse hammer equipped with a load cell at the tip.

In the ground-foundation tests, tests at different excitation points were carried out to calculate the full components of the impedance function matrix.

Shaking table tests were carried out applying seismic and sinusoidal waves. The shaking table has a size of 4m x 4m and it is capable of six degrees-of-freedom excitations.

The acceleration level for the sinusoidal excitation was kept constant with the amplitude of 20 gal. Excitation frequency range was 1~50Hz, with normal frequency intervals of 0.2Hz, and of 0.1Hz in the vicinity of the resonance frequency.

Based on the scale rule of the model, the time axis was multiplied by a factor of 1/3 and the duration time was set as 8.33 seconds in the seismic excitation. Figure 3 illustrates the time history of acceleration and its response spectrum. The input to the shaking table was modified applying the transfer function determined through the ground model tests to reproduce the wave illustrated in figure 3 at the ground surface level.

3 TEST RESULTS

3.1 Ground-foundation interaction test

Figure 4 illustrates the transfer functions for varied embedded depths in the impulse hammering tests for each ground model. Because the hammering pulse does not have enough power, the accelerometers could not catch accurate data in low frequency region. The disturbance near 0 Hz in the following figures is caused on this reason. In the figure, the transfer functions for the excitation applied to the top of the attachment are shown. Owing to the embedding of the foundation, peak amplitude decreases. There is also phase delay. The resonance frequency also increases slightly by embedding. These phenomena are clearer in soft ground model where the backfill material is same material as the ground material. These results mean the increase of the rigidity and the damping of the system with the increase of the embedment depth.

Figure 5 compares the transfer functions obtained by the shaking table tests with reference to embedment depth for each ground model. As a reference point of transfer function, the average of five points at pit bottom in each ground model is utilized. Owing to the embedding of the foundation, the amplification ratio decreases.

Figure 6 shows the rotational impedance functions obtained from the test results of the soft ground model. The impedance functions have many peaks which are caused by the reflected waves from the boundary of the model. Referring to the data processing method utilizing transient response (Mita, A. et al.), the reflected wave from the boundary can be removed.

Figure 7 shows an example of time history of the acceleration response of the base on the soft ground model. In the figure, at the point Δ , first arrival of the reflected wave from the boundary can be recognized. The durations are 0.1sec for the soft ground model and 0.04sec for the hard ground model. If data before the arrival of the first reflected waves are used to calculate the impedance functions, the impedance functions are regarded as those for the half space. The smooth impedance functions in figures 8 and 9 are those derived in this manner.

The imaginary part tends to increase with increasing embedment depth. The real part, in the full embedded case, decreases most sharply along with frequency axis, and the order of magnitude of the impedance function of each embedment depth changes as the frequency changes. However, in lower frequency region, the values of the impedance functions increase with embedment depth.

Figures 10 and 11 illustrate foundation input motions of each ground model. As a reference point of transfer functions, the average of five points at the pit bottom in each ground model is used. The horizontal component of the foundation input motion, in case of non embedded foundation on soft ground, has an amplitude of almost 1.0 and phase almost 0.0. However in the half embedded and full embedded cases, the amplitude decreases and

the phase is delayed from 10.0Hz on. Rotational components exist in all cases, but are largest in the non embedded case. If there is no pit, there should arise no rotational components in the non embedded case, therefore it is apparent that the pit has a significant effect on the foundation input motion. The decrease of amplitude with the embedment in higher frequency region is also seen in the hard ground model.

3.2 Ground-building interaction test

The transfer functions obtained by the hammering tests are compared in figure 12. In case of the soft ground model, the amplitude decreases to 1/3 by change from non embedded to half embedded, and again to 1/2 by change from non embedded to full embedded. From these observations, it is evident that the stiffness and damping ratio increase with embedment depth. While in the case of the hard ground model, peak amplitude does not decrease so much. From these observations, the damping ratio of the soil-structure interaction increases mainly in the case of soft ground model with embedment depth.

Sinusoidal and seismic excitations were also performed. Figure 13 compares the transfer functions with different embedment depths, with the average motion of five points in the bottom of the pit as a reference motion. Though in the case of the soft ground model the change of primary system frequency and amplification property are quite visible in the hammering test, their changes are not clear in the shaking table test for the soft ground model. In case of the hard ground model, the change of the amplitude with the change of embedment depth is not clear as well as the hammering test case.

The acceleration response spectra for seismic excitation in relation with embedment depth are shown in figure 14. The damping constant is set at 5%, and maximum acceleration is normalized to be 300gal at ground level in order to realize constant exciting level. The spectra at the building top decrease with the increase of the embedment depth and the peaks shift toward higher frequency both in soft and hard ground model.

Figure 15 shows the maximum response acceleration of the each floor of the model buildings. The maximum response value in the full embedded is smallest both in the soft ground and hard ground models. The acceleration responses of the hard ground model are much higher than those of the soft ground model.

The displacement mode ratio at the frequency where the transfer function phase comes to $-\pi/2$ first is shown in Table 2. As the embedment depth increases, the frequency increases, and the ratio of elastic deformation of the upper structure also increases. As the sway ratio of the embedded cases decreases, height of rotation center rises with increasing embedment depth. These phenomena are especially clear in the soft ground model.

4 CONCLUSIONS

Embedment effects on seismic response of a reactor building were verified experimentally using silicone rubber ground models with aluminum building models. From the ground-foundation tests, embedding their foundation is proved to increase impedance functions, especially their imaginary parts. Both the impedance function and the foundation input motion have shown complex frequency characteristics due to the reflected waves from the boundary of the ground model. However, a processing method which utilizes the transient response to eliminate the reflected waves, has been proved to allow us to simulate the impedance function and the foundation input motion for a uniform half space.

From the ground-building interaction tests, it has been verified that the embedment increases the primary system frequency and the ratio of elastic deformation at the top and decreases the response of the structure. It has been also found that the response of the structure on the soft ground is much smaller compared with that on the hard ground.

ACKNOWLEDGEMENTS

This work was carried out as the entrusted project sponsored by the Ministry of International Trade and Industry in Japan. This work was supported by "Sub-Committee of model test on Embedment Effect on Reactor Building" under "Committee of Seismic Verification Tests" of NUPEC. The authors wish to express their gratitude for the cooperation and valuable suggestion given by the members of Committee.

REFERENCES

- (1)Moriyama,K.et al. (1991), Comparison between Tests and Analyses for Ground-Foundation Models (Embedment Effect Test on Soil-Structure Interaction), 11th SMiRT.
- (2)Mita,A.et al. (1989), "Soil-Structure Interaction Experiment Using Impulse Response" EESD,Vol.18

Table.1 Material Properties of Ground Models

	soft ground	hard ground
Young's modulus E(kg/cm ²)	3.47	23.5
Poisson's ratio ν	0.49993	0.484
Shear wave velocity Vs (m/sec)	10.76	25.0
Density ρ	1.0	1.24
Damping factor h	0.03	0.01

Table.2 Displacement Mode Ratios at the Top of Test Models

(a) Soft Ground Model

Model	Embedment	Frequency* (Hz)	Sway (%)	Rocking (%)	Elastic Deformation (%)
Soft Ground + Building Model	Non-Embedment	8.1	20	52	28
	Half-Embedment	10.1	6	60	34
	Full-Embedment	13.5	0	20	80

*Frequency when the Phase Reaches $-\pi/2$ for the First time

(b) Hard Ground Model

Model	Embedment	Frequency* (Hz)	Sway (%)	Rocking (%)	Elastic Deformation (%)
Hard Ground + Building Model	Non-Embedment	15.6	6	20	74
	Full-Embedment	17.1	2	17	81

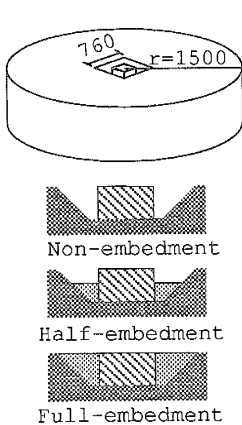


Fig.1 Ground and Foundation Models

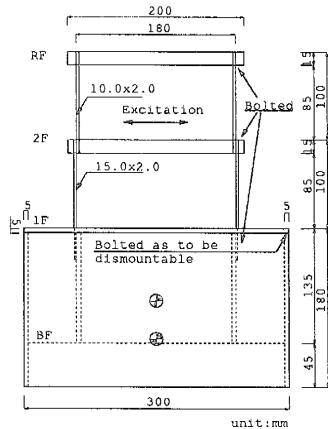


Fig.2 Reactor Building Model

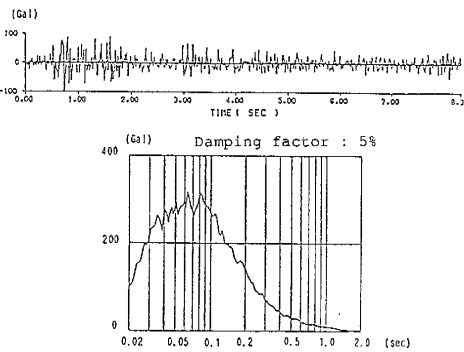


Fig.3 Time history of Acceleration and its Response Spectra

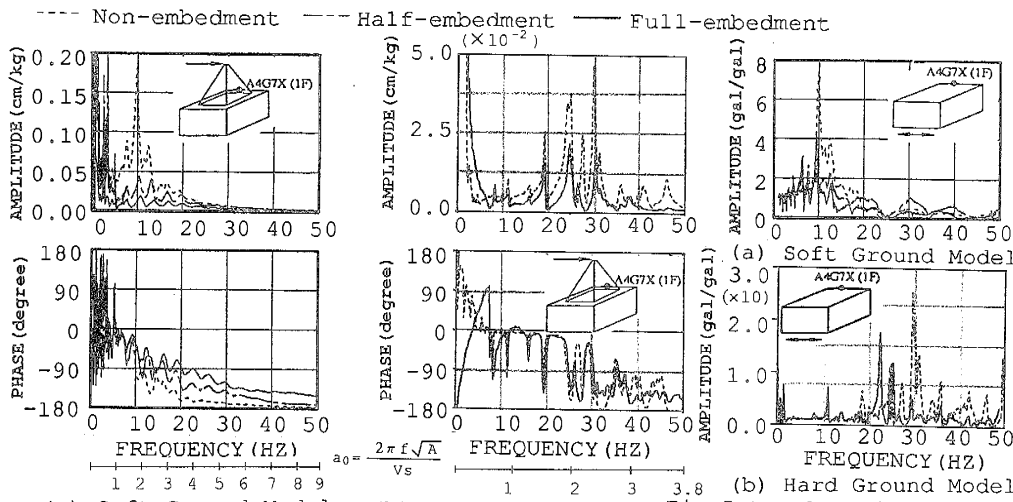


Fig.4 Displacement Transfer Functions for Hammering Tests Fig.5 Acceleration Transfer Functions for Sinusoidal Shaking Table Tests

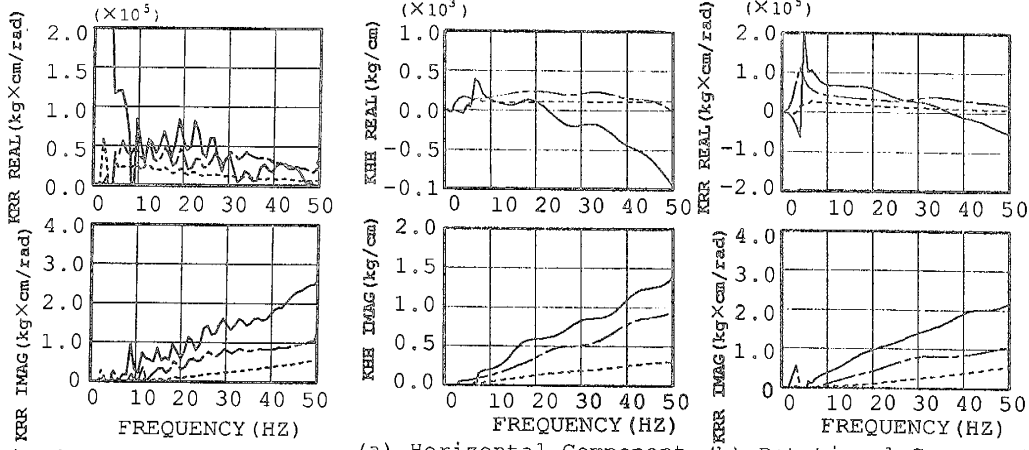


Fig.6 Rotational Component of Impedance Functions of Soft Ground Model Fig.8 Impedance Functions for half space (Soft Ground Model)

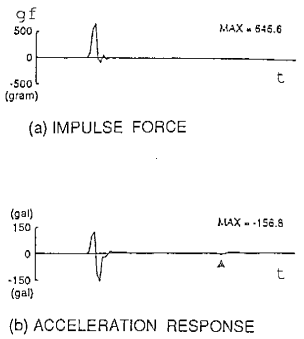


Fig.7 Time History of Response Wave in Hammering Test

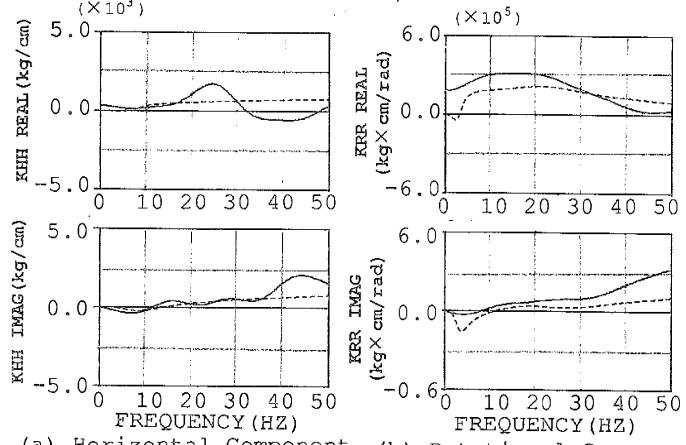
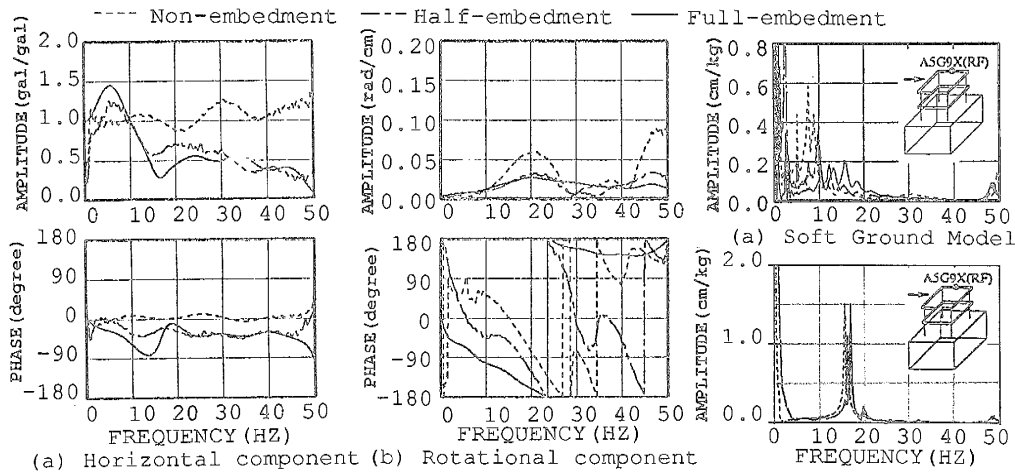
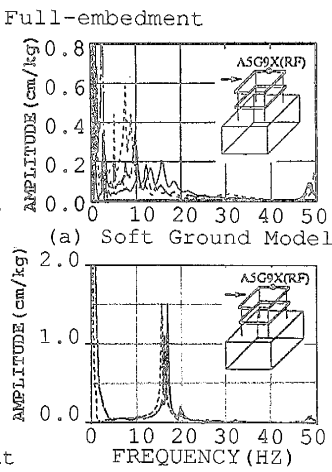


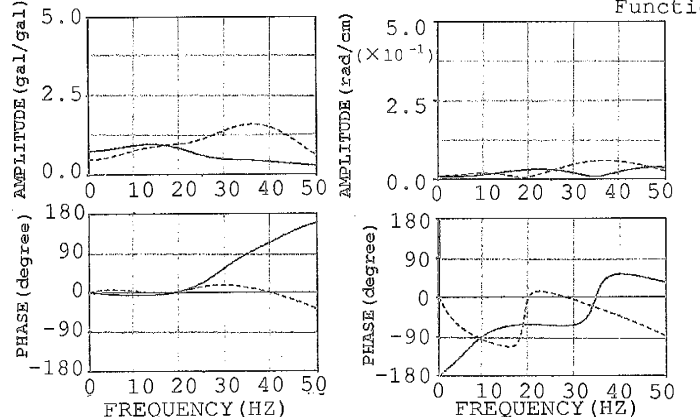
Fig.9 Impedance Functions for half space (Hard Ground Model)



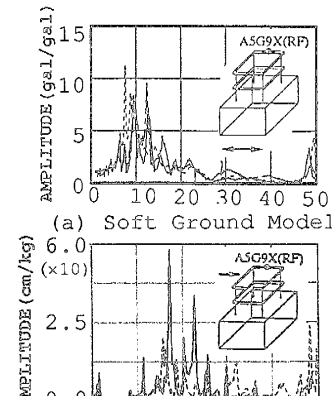
(a) Horizontal component (b) Rotational component



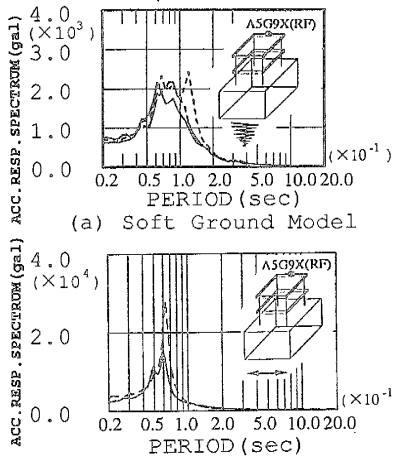
(a) Soft Ground Model (b) Hard Ground Model



(a) Horizontal component (b) Rotational component



(a) Soft Ground Model (b) Hard Ground Model



(a) Soft Ground Model (b) Hard Ground Model

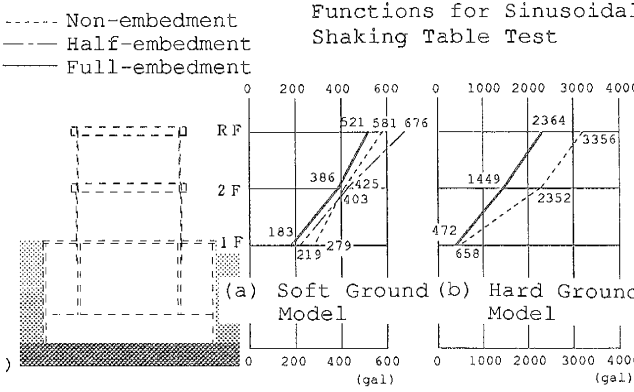


Fig. 15 Maximum Acceleration for Seismic Excitation